AVERAGE FLUXES FROM HETEROGENEOUS VEGETATED REGIONS

WIM KLAASSEN

Department of Physical Geography, University of Groningen, Kerklaan 30, 9751 NN Haren, The Netherlands

(Received in final form 18 June, 1991)

Abstract. Using a surface-layer model, fluxes of heat and momentum have been calculated for flat regions with regularly spaced step changes in surface roughness and stomatal resistance. The distance between successive step changes is limited to 10 km in order to fill the gap between micro-meteorological measurements and meso-scale models. A single-layer 'big leaf' model of the vegetation is compared with a multi-layer model to assess the performance of the former in the determination of surface fluxes in heterogeneous terrain.

The sub-models of vegetation and atmosphere are mainly based on well-known theory. However, a modification of the mixing-length closure of atmospheric exchange is included to achieve a more realistic calculation of fluxes near step changes at the surface. Measurements, presented in the literature, are used to determine the mixing-length parameters and to validate the calculated fluxes downwind of a change in vegetation cover.

The single-layer model, well validated for homogeneous surfaces, underestimates the effects of local advection upon the surface fluxes as this model neglects air flow across the edges of tall vegetation. Using the multi-layer model, local advection results in an increase of up to 50% in regional momentum flux and smaller changes in regional evaporation. Even widely spaced heterogeneities appear to influence regional fluxes.

1. Introduction

The surface fluxes of sensible and latent heat and momentum are important boundary conditions for climate studies. These fluxes can be calculated from surface characteristics (roughness and wetness), the available energy, and atmospheric properties (wind velocity, temperature and humidity). A problem arises when the surface conditions vary horizontally. In those cases, the atmospheric properties slowly adjust to surface changes, and the average flux over a region may deviate from the flux obtained from regionally averaged surface and atmospheric conditions, or even that obtained from the actual surface and regionally averaged atmospheric conditions. The general objective of this study is to find a method to determine average fluxes from a heterogeneous region.

The averaging problem appears at all scales, as surface inhomogeneities occur at scales ranging from a single leaf to a region (Jarvis and McNaughton, 1986), up to the whole earth. Irregularities at the smallest scales of leaves and plants are averaged out by measurements at the usual micro-meteorological scale. At a larger scale, Shuttleworth (1988) distinguishes organized and disorganized heterogeneities. An organized heterogeneity, with a horizontal length scale of at least 10 km, results in a coherent response of the atmosphere at the meso-scale. The

Boundary-Layer Meteorology **58**: 329–354, 1992.

organized heterogeneities have been studied through aircraft measurements and meso-scale modelling in several international projects, like HAPEX (André *et al.*, 1986) and FIFE (Betts *et al.*, 1990).

For the smaller scale 'disorganized' heterogeneities, Avissar and Verstraete (1990) suggest that one calculates average fluxes from a regionally constant boundary layer. Close to the surface however, the heterogeneities create internal boundary layers with varying atmospheric conditions. According to André *et al.* (1990) "sharp transitions at scales between 1 and 10 km are particularly harmful for the present strategy" of surface flux averaging based on a regionally constant boundary layer.

The specific objective of the present study is to determine average fluxes of heterogeneous regions of up to 10 km length scale. The fluxes are calculated using a high resolution surface-layer model. The region is assumed to be flat with heterogeneity arising from varying vegetation. A similar approach has been used by Mason (1988) for momentum flux and by Claussen (1991) for heat flux. Both studies show that the average momentum flux of a heterogeneous region is increased by local advection.

Mason (1988) and Claussen (1991) both represent the vegetation by a single layer with all air moving above the vegetation. The single-layer 'big leaf' model (Monteith, 1965) is well validated for flux calculations over homogeneous surfaces. However, the single-layer model does not account for air flow crossing the edges of tall vegetation. Consequently, the single-layer model may be invalid for flux calculations near vegetation changes. As a secondary objective, this study aims to examine the validity of the single-layer vegetation model for flux calculations of heterogeneous regions.

In order to test the single-layer model, the resulting fluxes are compared to the results of a multi-layer model of vegetation. The multi-layer model is based on the model of Li *et al.* (1985) because of its simplicity. In their model, Li *et al.* (1985) describe the atmospheric exchange with a first-order mixing-length closure assumption and an extension for counter-gradient transport within vegetation. The mixing length is expected to depend on the zero-plane displacement of the vegetation, resulting in horizontal variations of the mixing length in heterogeneous terrain. In a more recent paper, Li *et al.* (1990) estimate these variations in mixing length from a prescribed linear adjustment. In the present study a more physically based estimation of the mixing length is developed. New parameters in the mixing length formulation are determined from published measurements. Finally, both the single- and multi-layer mode are validated on other published data.

The study has benefited from the experience of our research group in determining forest evaporation. Starting with the one-dimensional approach (Veen and Dolman, 1989), studies have been extended to measure fluxes near a forest edge (Kruijt *et al.*, 1991) and to determine atmospheric conditions above forests from standard meteorological data (Hutjes *et al.*, 1991). The present study intends to generalise the results of the former studies.

2. Theory

2.1. General description of the surface-layer model

The model has been set up to determine the influence of surface heterogeneity on regionally averaged fluxes of heat and momentum. A heterogeneous region is represented by two adjacent homogeneous zones. The zones have distinct surface characteristics, in particular aerodynamic roughness and stomatal resistance. The surface-layer model is run in two versions, the single-layer and multi-layer model version. Using the single-layer model, the surfaces of both zones are represented by single layers, each with a horizontally constant roughness length z_0 and stomatal resistance r_s. Generally, zones have been chosen that vary widely in roughness or vegetation height. Using the multi-layer model, the surface of the smoother zone is still represented by a single layer, but the surface of the rougher zone is then represented by a multi-layer vegetation model with horizontally constant leaf area density and stomatal resistance.

The surface types are assumed to be of infinite width in the direction perpendicular to the wind in order to make a two-dimensional approach possible. A vertical column of air is simulated to move over the region. By assuming stationarity, the two-dimensional flow is calculated from the time variations in the one-dimensional column.

As long as the atmosphere is unadjusted to the underlying surface, the wind velocity, temperature, and humidity change when the air moves over the surface. At the same time, the surface fluxes deviate from their adjusted values. These advective processes can be separated according to scale into regional and local processes (Brakke *et al.*, 1978). As this study aims to quantify local advection, the regional component should be minimized. This is done by iteration over a large sequence of identical regions until the air is adjusted to the heterogeneous region and the properties of in- and out-flowing air have converged. The procedure is equivalent to Fourier analysis (Mason, 1988), which is also based on an infinite extension of identical regions.

2.2. Fluxes from a single-layer canopy

Using the single-layer model version, fluxes are calculated from standard flux-profile relations to the first level (height z_1) in the atmosphere. The vertical momentum flux, or surface stress, τ is given by:

$$\tau = \rho u_*^2 \tag{1}$$

with $u_* = uk/\ln(z_1/z_0) - \Psi_m$, where ρ is air density (kg m^{-3}), u_* the friction velocity (m/s), u the wind velocity (m/s) at height z_1, z_0 the roughness length (m) of the surface, Ψ_m a stability function and k is von Karman's constant, taken as 0.4. The stability functions Ψ and Φ (Equations (18)–(20)) are taken from Webb (1970, 1982), following Garratt and Pielke (1989).

The fluxes of sensible and latent heat H and λE are given by:

$$H = \rho c_p (T_s - T_a)/r_a \tag{2}$$

$$\lambda E = \rho c_p/\gamma (e_s^* - e_a)/(r_a + r_s) \tag{3}$$

where c_p is the specific heat of the air at constant pressure ($c_p = 1005$ J/kg), λ the latent heat of vaporization ($\lambda = 2.5 \times 10^6$ J/kg), γ the psychrometer constant ($\gamma = \rho c_p/(0.622\lambda) \simeq 66$ Pa/K), T the temperature, $e(*)$ the (saturated) water vapour pressure and r the resistance; the subscripts (s) and (a) refer to the surface and air, although the surface resistance will be denoted as 'stomatal resistance'. By combining (2), (3) and the energy balance:

$$R_n - G = A_\epsilon = \lambda E + H \tag{4}$$

where R_n is the net radiation, G the ground heat flux and A_ϵ the available energy (all W/m^2), Monteith (1965) showed that:

$$\lambda E = \frac{sA_\epsilon + \rho c_p (e_a^* - e_a)/r_a}{s + \gamma (r_a + r_s)/r_a}, \tag{5}$$

where s is the slope of saturated water vapour pressure with temperature (Pa/K).

Some results will be explained using the concept of equilibrium evaporation (λE_{eq}) that is obtained from (5) by taking the limit to infinite atmospheric resistance (McNaughton, 1983):

$$\lambda E_{eq} = A_\epsilon/(1 + \gamma/s)\,. \tag{6}$$

Please note the difference in this study between equilibrium (no turbulence) and adjusted (no advection, i.e., after a very long fetch) evaporation. Actual evaporation will equal equilibrium evaporation when the atmospheric humidity deficit equals some surface-dependent value denoted as 'equilibrium humidity deficit' (McNaughton, 1983). Where the humidity deficit deviates from its equilibrium value, evaporation will deviate from its equilibrium value as well. At a given humidity deficit, the deviation from equilibrium evaporation will increase with decreasing atmospheric resistance.

The net radiation is calculated from the radiation balance:

$$R_n = (1 - \alpha)R_s + \epsilon(R_l - \sigma T_s^4)\,, \tag{7}$$

where R_s and R_l are the incoming shortwave and longwave radiation, α the albedo and ϵ the emissivity of the surface, and σ is the Stephan-Boltzmann constant ($\sigma = 5.67 \times 10^{-8}$ W m^{-2} K^{-4}). Equation (7) is used because incoming radiation can often be assumed constant within the region, whereas net radiation depends on surface characteristics.

The ground heat flux is taken as $G = 0.1R_n$ for agricultural crops (de Bruin and Holtslag, 1982) and $G = 0.036R_n$ for forest (Baldocchi *et al.*, 1984). The atmospheric resistance is obtained from the heat transfer relation with

$$r_a = (\ln(z_1/z_{0h}) - \Psi_h)/\mathrm{k}u_* \tag{8}$$

where z_{0h} is the roughness length for heat, taken as $z_{0h} = z_0 \exp(-2)$ (Garratt and Francey, 1978).

2.3. Fluxes from a multi-layer canopy

The multi-layer canopy model is kept simple as it only serves to analyse the influence on the surface fluxes of air inflow and outflow near inhomogeneities. The free model parameters are varied until the surface fluxes agree with the single-layer model in adjusted flow (i.e., after an infinitely long fetch). The canopy is divided into a number of height intervals Δz with leaf area density A_1. The surface flux is defined as the sum of the fluxes for each layer.

The drag force of leaves in a layer is given by:

$$F_d = 0.5 \times 0.16 A_1 u^2 . \tag{9}$$

The factor 0.5 arises because the leaf area perpendicular to the flow is only half of the total (one-sided) leaf area for a regular leaf angle distribution. The factor 0.16 takes into account the shelter effect of clustered leaves (Raupach and Thom, 1981).

A countergradient force F_{cg} is included for countergradient transport in vegetation. Due to the countergradient force, a higher and more realistic wind velocity is simulated within the canopy, resulting in a more stable calculation of the atmospheric flow. According to Li *et al.* (1985), F_{cg} is given by:

$$F_{cg} = \frac{0.04\{u(h_c) - u(z)\}z}{1 + 0.8 A_1 h_c} , \tag{10}$$

where z is the height within the canopy (m) and h_c the canopy height (m).

The sensible and latent heat source strengths H_s and E_s are basically given by Equations (2)–(6), but now the available energy in a layer is given by:

$$A_\epsilon = R_n(z + \Delta z) - R_n(z) = R_n(z + \Delta z)\{1 - \exp(-K_R A_1 \Delta z)\} , \tag{11}$$

where K_R is the extinction coefficient for net radiation, taken as 0.5 (Jarvis and Leverenz, 1983).

The atmospheric resistance is now defined as the resistance between the leaves and the surrounding air, and is given by:

$$r_a = 90/(A_1 \Delta z)(l_w/u)^{0.5} , \tag{12}$$

where l_w is the effective leaf width (m), taken as 0.05 m; the factor 90 takes leaf shading into account (Pearman *et al.*, 1972; Spittlehouse and Black, 1982).

The stomatal resistance increases with depth in the canopy and is taken to be inversely proportional to net radiation at that level:

$$r_s = r_{so} R_n(h)/(R_n(z + \Delta z) A_1 \Delta z) , \tag{13}$$

where r_{so} is a free parameter in the model that determines the overall level of transpiration.

2.4. Atmospheric flow

The surface fluxes depend on wind velocity, temperature and humidity of the air; the latter variables, in turn, depend on the surface fluxes. The horizontal variations in these variables are calculated from the conservation laws:

$$u\frac{\delta u}{\delta x} + w\frac{\delta u}{\delta z} = \frac{\delta \tau}{\rho\,\delta z} - F_d + F_{cg}\,, \tag{14}$$

$$u\frac{\delta \theta}{\delta x} + w\frac{\delta \theta}{\delta z} = \frac{1}{\rho c_p}\left\{\frac{\delta H}{\delta z} + H_s\right\}, \tag{15}$$

$$u\frac{\delta q}{\delta x} + w\frac{\delta q}{\delta z} = \frac{1}{\rho}\left\{\frac{\delta E}{\delta z} + E_s\right\}. \tag{16}$$

where δ is the local derivative and w the vertical wind velocity (m/s), θ the potential temperature (K), q the specific humidity (−). The coriolis force and local pressure perturbations have been neglected. The coriolis force is not important for this small-scale study and the omission of pressure perturbations is discussed in Sections 2.5 and 3. To use Equations (14)–(16), mathematical descriptions are needed for w and the fluxes τ, H and E.

Vertical wind velocity is calculated from the continuity equation of an incompressible fluid:

$$\frac{\delta u}{\delta x} + \frac{\delta w}{\delta z} = 0\,. \tag{17}$$

Momentum flux is calculated from the friction velocity using Equation (1) in its differentiated form:

$$u_* = l_m \frac{\delta u}{\delta z}\Phi_m^{-1}\,. \tag{18}$$

Atmospheric fluxes of sensible and latent heat are given by:

$$H = \rho c_p \frac{u_* l_m}{\Phi_h}\frac{\delta \theta}{\delta z}\,, \tag{19}$$

$$E = \rho \frac{u_* l_m}{\Phi_h}\frac{\delta q}{\delta z}\,, \tag{20}$$

where l_m is the mixing length. A realistic formulation of the mixing length is essential to obtain accurate fluxes. The simplest formulation is $l_m = kz$, which is realistic close to the surface in adjusted flow, and is used for the first height level

in the single-layer model (Equation (1)). At larger heights, a slightly different formulation is used to limit the mixing length (Blackadar, 1962):

$$l_{ma} = kz/(1 + kz/l_{mm}) , \tag{21}$$

where l_{ma} is the adjusted mixing length that is found after an infinite fetch over a homogeneous surface, and l_{mm} is the maximum mixing length, taken as 40 m. Within vegetation, a correction upon (21) is necessary to find a realistic roughness length and zero-plane displacement. The correction is derived by differentiating (21):

$$l_{ma}(z + \delta z) = l_{ma}(z) + \delta l_{ma}/\delta z \tag{22}$$

with

$$\frac{\delta l_{ma}}{\delta z} = k\left(1 + \frac{l_{ma}/l_{mm}}{1 - l_{ma}/l_{mm}}\right)^{-2} .$$

Within vegetation, the flow of air around the obstacles (leaves and stems) results in the production of small-scale eddies and an absorption of large eddies (Baldocchi and Meyers, 1988). The conversion of turbulence to smaller scales is simulated by a reduction of mixing length according to:

$$l_{ma}(z + \delta z) = [l_{ma}(z) + \delta l_{ma}/\delta z] \exp(-K_1 A_1) , \tag{23}$$

where K_1 is the reduction coefficient for mixing length by leaves. K_1 is estimated from the roughness length and zero-plane displacement, as described in Section 2.5. Equation (23) is in good agreement with the formulation of Li *et al.* (1985). By varying the gradient of l_{ma}, instead of l_{ma} directly, only one equation is needed to calculate the adjusted mixing length within and above vegetation. Equation (23) is used to calculate the adjusted mixing length from the surface upwards with $l_{ma} = 0$ at $z = 0$.

The adjusted mixing length changes suddenly at the edges of tall vegetation, due to a sudden change in leaf area density. These changes would result in unrealistic changes in the calculated atmospheric fluxes. Horizontally smooth variations of the actual mixing length l_m are simulated in the present study from advection ($\delta l_{mv}/\delta x$) and adjustment ($\delta l_{mj}/\delta x$):

$$\frac{\delta l_m}{\delta x} = \frac{\delta l_{mv}}{\delta x} + \frac{\delta l_{mj}}{\delta x} . \tag{24}$$

Advection of mixing length from a different height level arises from:

$$\frac{\delta l_{mv}}{\delta x} = \frac{w}{u}\frac{\delta l_m}{\delta z} . \tag{25}$$

Adjustment of mixing length is estimated empirically by:

$$\frac{\delta l_{\mathrm{mj}}}{\delta x} = c_1(1 - l_m/l_{\mathrm{ma}}) , \tag{26}$$

where c_1 is the 'rate of adjustment' constant, whose estimation is described in Section 2.5. It might be possible to describe the horizontal variations of mixing length with adjustment only, but advection is included because it is expected to improve the accuracy of the mixing-length estimation for the following reasons: (1) Equation (25) gives a physically plausible cause for horizontal variations of the mixing length, and (2) the vertical transport of air near edges of vegetation approximates the change in zero-plane displacement, so advection may describe the main part of the variations in mixing length that are encountered near vegetation edges.

2.5. Determination of free parameters of the mixing-length parameterisation

Two constants of the mixing-length parameterisation need to be determined: the reduction coefficient for mixing length by leaves, K_1 (Equation (23)), and the 'rate of adjustment' constant of mixing length, c_1 (Equation (26)).

The reduction coefficient K_1 determines the adjusted mixing length within and just above tall vegetation and consequently the zero-plane displacement d and roughness length z_0 of the vegetation. d and z_0 have been calculated as a function of K_1 for rice and for forest from the simulated wind profile at very long fetch. A neutral stratification has been assumed, as well as an infinite maximum mixing length, in order to obtain a logarithmic wind profile. The leaf area densities of forest and rice are given in Table I.

The results are shown in Figure 1. For $K_1 = 0$ we find $d = 0$ and a large roughness length as the turbulence can effectively penetrate the vegetation. In this case, the largest relative roughness length is found for forest, as a larger leaf area index results in more drag. For increasing K_1, an increasing d and decreasing z_0 are obtained. At given K_1, an increasing leaf area density results in a further reduction in mixing length and thus in an increased zero-plane displacement. The reduced mixing length also results in a reduced exchange between different height layers. Therefore, the wind velocity within the canopy decreases and the reduced wind drag results in a decreased roughness length. The sensitivity of z_0 and d to leaf area density is in good agreement with the theoretical study by Shaw and Perreira (1982). The dependence on leaf area density complicates the comparison to observational studies, as the distribution of leaf area density is rarely measured in connection with measurements of z_0 and d. The leaf area densities of Table I are assumed to be representative for the following observational studies.

Jarvis *et al.* (1976) compared z_0 and d measurements of 15 coniferous forests; the statistical analysis of these data by Shuttleworth (1989) showed $z_0/h_c = 0.076 \pm 0.047$ and $d/h_c = 0.78 \pm 0.09$, where h_c is the height of the canopy. This result is most accurately simulated with $K_1 = 0.6$. The values for agricultural crops:

TABLE I

Input data for the simulation of two heterogeneous regions

1.1. *Data for the whole region*				
Region characterisation	RICE		FOREST	
Surface layer height h_s (m)	100		200	
Wind velocity at h_s (m/s)	4		10	
Temperature at h_s (°C)	21		20	
Relative humidity at h_s (%)	40		70	
Incoming shortwave radiation ($W m^{-2}$)	350		600	
Incoming longwave radiation ($W m^{-2}$)	350		350	
1.2. *Data for the first zone* in multi-layer parameterisation				
Leaf area density versus height	z (m)	A_1 (m^{-1})	z (m)	A_1 (m^{-1})
	0.25	1.4	1.5	0.3
	0.5	5.0	2.5	0.3
	0.75	5.7	3.5	0.5
	1.0	2.6	4.5	0.6
			5.5	1.0
			7.0	1.0
			8.5	1.0
			10	0.5
Leaf area index ($m^2 m^{-2}$)	4.0		6.0	
Stomatal resistance factor r_{so} ($s m^{-1}$)	93		165	
1.3. *Data for the first zone* in a single-layer parameterisation				
Albedo	0.20		0.10	
Emissivity	0.98		0.98	
Roughness length (m)	0.13		0.9	
Stomatal resistance ($s m^{-1}$)	50		58	
1.4. *Data for the second zone*				
Characterized by	bare soil		heath/AC*	
Albedo	0.20		0.20	
Emissivity	0.98		0.98	
Roughness length (m)	0.003		0.03	
Stomatal resistance ($s m^{-1}$)	10 000		30	

*AC is agricultural crop.

$z_0/h_c = 0.13$ and $d/h_c = 0.63$ (Monteith, 1973) are most accurately simulated for $K_1 = 0.5$. For further simulations, $K_1 = 0.5$ is used.

The 'rate of adjustment constant for mixing length', c_1, determines the rate at which turbulence adjusts to its equilibrium value. Turbulence primarily influences the momentum exchange, so c_1 can be determined from drag measurements in an unadjusted flow. In the present study the experiments by Bradley (1968) of surface drag after a step change in surface roughness (Figure 2) are used. After the transition to a rougher surface, the flow decelerates, moves upward (Equation (17)) and advects a smaller mixing length (Equation (25)). The mixing length adjusts almost immediately to the equilibrium value for $c_1 = 1$; this situation approaches the results using a fixed mixing length. The fetch for adjustment of mixing length increases for decreasing c_1. The measurements of Bradley suggest

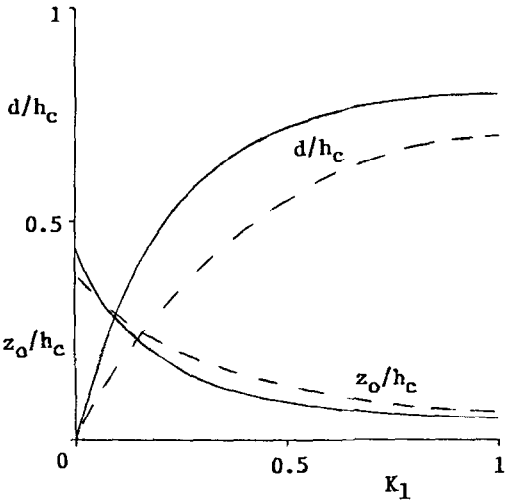

Fig. 1. Simulated roughness and zero-plane displacement, relative to the canopy height, versus the extinction coefficient for mixing length by leaves, ---- = rice and —— = forest.

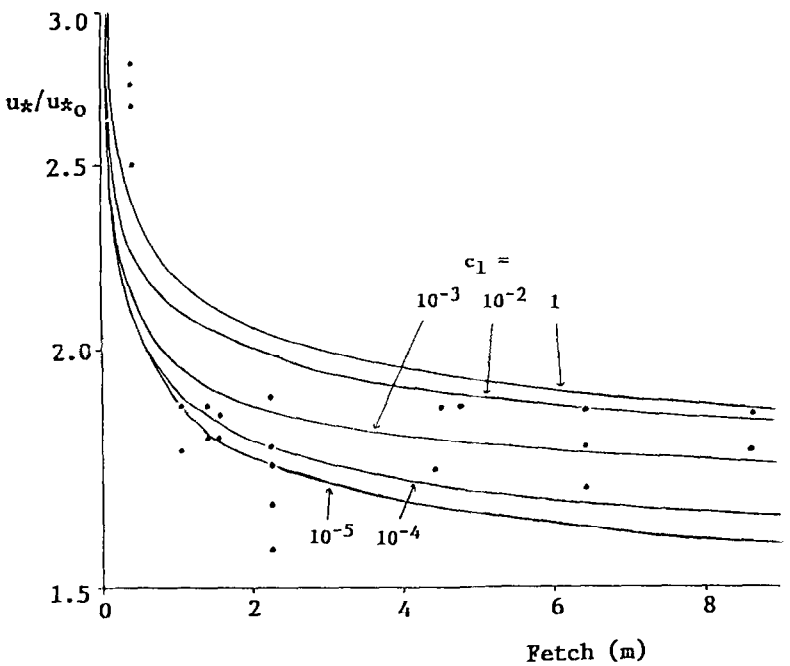

Fig. 2. Simulated surface friction velocity relative to the upstream value after a smooth-rough surface transition versus fetch for several values of the constant for adjustment of mixing length compared to Bradley's (1968) data.

hardly any adjustment of mixing length during the first 2 m, then followed by a rather quick adjustment. Assuming a constant c_1, the best overall agreement is obtained for $c_1 = 10^{-3}$. Some overestimation of wind velocity and drag close to the smooth-rough transition may result from the neglect of pressure perturbations.

By comparing the results for $c_1 = 10^{-3}$ with those of Claussen (1988), it appears that the present model has a performance comparable to that of the E-ϵ model. The similarity with the E-ϵ model is based on similar advection equations for kinetic energy (in the E-ϵ model) and mixing length (in the present study). However, mixing-length closure is much simpler since (1) fewer equations have to be solved during the calculations, (2) fewer empirical constants (k and c_1, as well as K_1 in the case of a multi-layer vegetation) enter the equations, and (3) the effects of atmospheric stability and reduction of mixing length within vegetation can be more straightforwardly incorporated.

3. Observations

The surface-layer model is validated on published measurements of surface fluxes downwind of a sudden change in vegetation cover. The data of Gash (1986), obtained near a heath-forest interface and denoted as G86, are used for the momentum flux, because air flow into and from vegetation is largest for a tall canopy such as forest. Heat flux variations near forest edges have not yet been published, so observations from a lower canopy are used. The data of Lang *et al.* (1974), denoted as L74, on irrigated rice are used because the latent heat flux was obtained from lysimeter observations which are not affected by uncertainties in eddy diffusivities during advective conditions (Lang *et al.*, 1983).

3.1. Input data

The input data for the model are shown in Table I. Note that a heterogeneous region is composed of two zones; here irrigated rice and dry bare soil for the 'rice' region, and forest and heath or agricultural crops (AC) for the 'forest' region.

The surface-layer height is the upper boundary of the model; at this height the average values of the atmospheric variables above the region (wind, temperature and humidity) are defined. At the upper boundary, a 'matched load' (Crout *et al.*, 1990) enables the variables and fluxes to change as if the surface layer extended to infinite height.

The atmospheric variables for rice are the average values of the first three measuring days of L74; the fourth day is omitted as the fetch was poorly defined. Temperature and radiation values of L74 are small compared to G86, because the observations are averaged over 24 h. The data of G86 were measured in winter when heat fluxes are very small. Consequently, the atmospheric stratification can be assumed to be neutral for the validation experiment. For the regional simulations of Section 4, however, typical midday summer conditions are used to extend the analysis of momentum to heat fluxes.

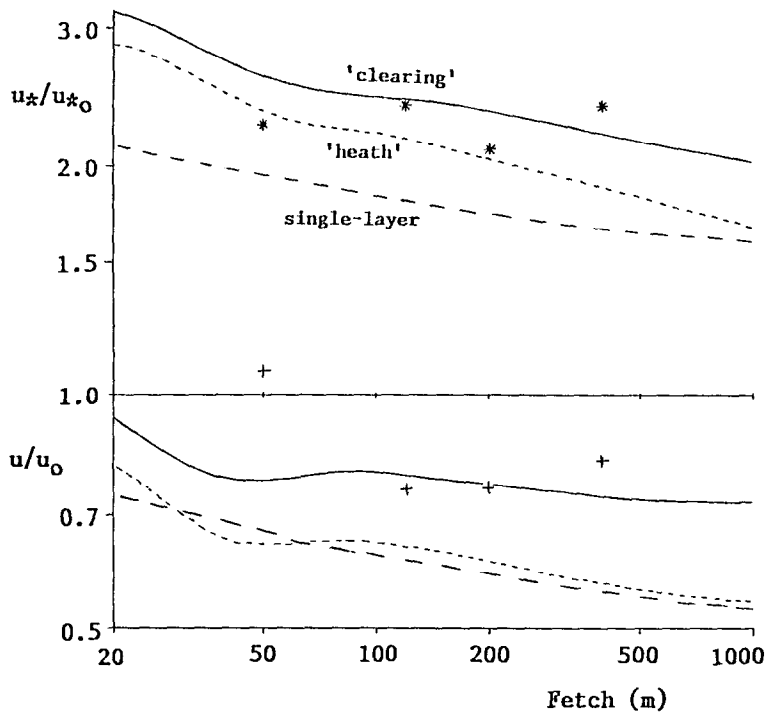

Fig. 3. Simulated wind velocity (below) and friction velocity (above) above forest after a heath-forest transition relative to their upstream values versus fetch compared to Gash's (1986) data, —— = multi-layer model initialised to a clearing of 1 km in a large forest (see text), ----- = multi-layer model initialised to heath, – – – – = single-layer model, + = measured wind velocity (normalized) and * = measured friction velocity (normalized).

The model uses stomatal resistances as input parameters; as these were not measured in the experiments of L74 and G86, they have been estimated from the resulting transpiration in the following way: The stomatal resistance of rice is determined from $\lambda E/R_n = 1.15$ after 300 m fetch (L74). The high resistance of bare soil is chosen arbitrarily and results in a very small latent heat flux from the dry soil. The short vegetation of G86 consisted of heath; for the simulations of Section 4, the stomatal resistance factor is estimated from agricultural canopies (AC), because the rate of transpiration is better known for these canopies. The stomatal resistances for forest and AC were iterated until $\lambda E/R_n = 0.6$ for forest (Verma *et al.*, 1986) and $\lambda E/R_n = 0.8$ for AC (Kim *et al.*, 1989). Note that despite the different Bowen ratios of forest and AC, similar transpiration results, because differences in albedo and surface temperature result in a different net radiation and sensible heat flux. A similar difference between forest and cereals was used by Pinty *et al.* (1989) in the situation of adequate soil water availability.

3.2. Validation

Wind and friction velocities after a heath-forest transition are shown in Figure 3. The measured data were scaled with their upwind values. The heath-forest transi-

tion is simulated using two different initial conditions. One version, denoted by 'heath', is initialised with a wind profile that is fully adjusted to heath. The 'clearing' version is initialised with a wind profile that is adjusted to forest before the wind enters a clearing of 1 km heath and flows into the forest again. Using this version, the data for the clearing are obtained 400 m upwind of the forest edge, in agreement with G86. The multilayer model has been run for 'heath' as well as a 'clearing', the single-layer model for 'clearing' only.

The 'clearing' and 'heath' situations show differences in the relative wind and friction velocities; in fact both versions result in almost equal velocities above forest, but deviate above heath. These differences show that although the lowest level of the atmosphere is quickly adjusted to heath as concluded by G86, the wind and friction velocities in an extended clearing deviate from a truly open field situation. According to the model, the decreased velocities in the clearing are related to vertical flux divergence above the measurement level. The model validation is restricted to the 'clearing' situation.

Figure 3 shows good agreement between the multi-layer forest model and the measured wind and friction velocities, except for the wind velocity at the smallest fetch. The deviation at small fetches is probably influenced by the neglect of pressure perturbations in the model. The single-layer model version clearly underestimates both velocities, as discussed below.

After a forest-heath transition (Figure 4), the wind and friction velocities are strongly overestimated when using the single-layer version. The deviations of the single-layer model after both transitions are explained by the neglect of air flow into, and from, the stem space of tall vegetation. The overestimation of velocities after a forest-heath transition are caused by the neglect of slowly moving air that emerges from the stem space. Underestimation of both velocities after a heath-forest transition is caused by the neglect of air moving into the stem space, implying that air from a larger height with higher wind velocity enters the crown (where most of the exchange with the surface takes place).

The multi-layer model accurately simulates the wind velocity after the forest-heath transition (Figure 4). The friction velocity is simulated well for long fetches but is less than the observed values for short fetches. However, as the observations were not corrected for vertical wind (Gash, pers. comm.), the flux observations at small fetches are not useful for validation.

The simulation of latent heat flux is validated on lysimeter measurements of Lang *et al.* (1974) at an irrigated rice canopy in a semi-arid region. In order to compare observations of different days, the data have been scaled with the average value over the field. Measurements and simulations show a strong and similar dependence of transpiration on fetch (Figure 5), although the observations show a large scatter. The single- and multi-layer model versions result in almost identical transpiration values after 50 m of fetch. In the first metres, the transpiration in the multi-layer version is higher, because of the larger transpiring leaf area. Especially at small fetches, the simulated transpiration exceeds the available energy, resulting in a stable atmospheric layer just above, as well as in the upper

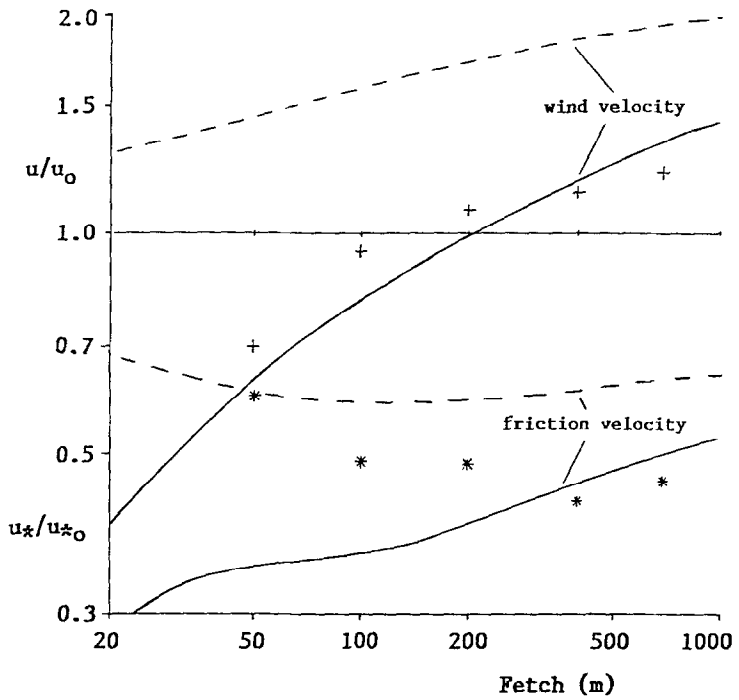

Fig. 4. As Figure 3, but for a forest-heath transition and the models initialised to forest.

part of the canopy. The stable layer suppresses the atmospheric exchange, resulting in only small differences between the multi- and single-layer model versions.

4. Simulated Regional Fluxes

Based on the observations of L74 and G86, two data sets are given in Table I for further simulations. The measurements have been generalized by varying the scale of the region (l_r = region length, i.e. the downwind length of both zones) and the fractional cover f of the tallest canopy within the region. The model has been run until regional adjustment of the flow was obtained (see Section 2.1), in order to quantify the regional consequences of local advection.

4.1. Partially forested regions

Transpiration versus fetch of a partially forested region is shown in Figure 6. Note that the air has just blown over AC before it enters the forest at the left part of the figure.

The simulated transpiration of both surfaces (forest and AC) falls below the value that would occur if the air had been fully adjusted to these surfaces. The deviations from adjusted evaporation that are found at limited fetches after the transition are primarily caused by variations in the atmospheric exchange or fric-

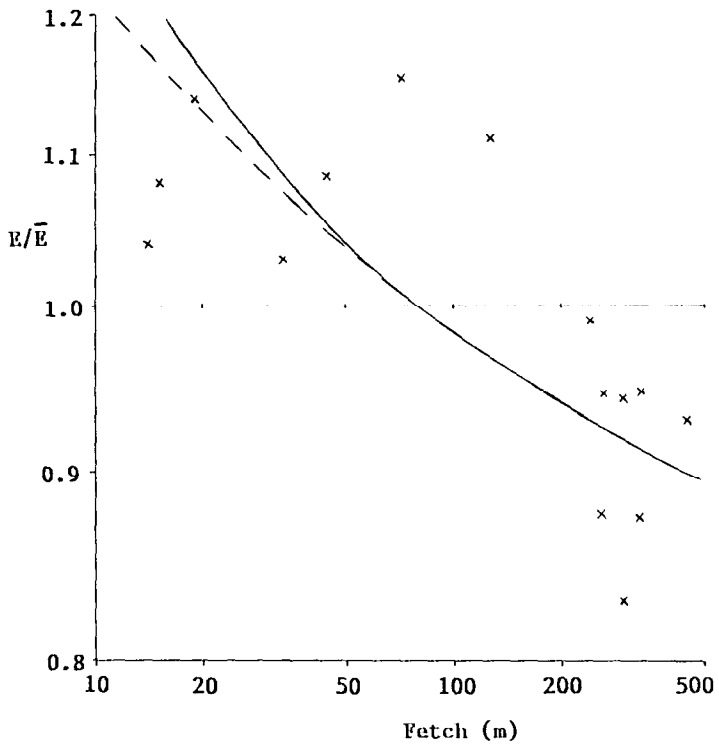

Fig. 5. Simulated transpiration of an irrigated rice field in a semi-arid region versus fetch, compared to data of Lang *et al.* (1974). The data are relative to the average over 500 m fetch. —— = multi-layer model and ---- = single-layer model.

tion velocity. An increase of friction velocity results in an increasing deviation from equilibrium evaporation. At the temperatures in this simulation, λE_{eq} equals $0.7(R_n - G)$, so evaporation from the forest is below the equilibrium rate and the evaporation of AC slightly above equilibrium.

At small fetches above forest, the friction velocity is increased above the adjusted value (Figure 3), resulting in a larger deviation from equilibrium evaporation or a decrease of latent heat flux in this case. This effect is most pronounced for the multi-layer model, as this model simulates the largest and most realistic increase in friction velocity.

At small fetches above AC, the friction velocity is below the adjusted value so evaporation will further approach the equilibrium value, or decrease in this case. This effect is small as the evaporation hardly exceeds the equilibrium value. A larger effect is caused by the reduction of available energy. The decreased friction velocity results in increased resistances to heat; at a given surface temperature, the increased resistance would decrease both heat fluxes. The surface temperature increases to close the energy balance (Equation (4)), so the surface emits more longwave radiation and net radiation (Equation (7)) and available energy de-

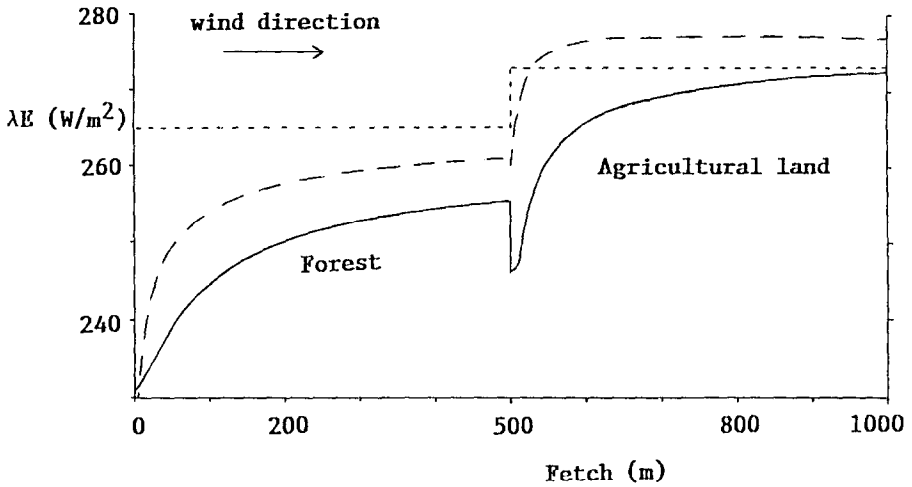

Fig. 6. Transpiration versus fetch for a region of 0.5 km forest and 0.5 km agricultural land: the region is surrounded by equal regions, resulting in a transition from agricultural land to forest at the left side of the figure. —— = multi-layer model, – – – – = single-layer model and ---- = without local advection, by assuming that the air is immediately adjusted to the underlying surface up to the upper boundary at 200 m height.

creases. As a result, the decreased friction velocity still results in a decrease of both heat fluxes. This effect at AC is most pronounced when the atmospheric exchange is simulated with a multi-layer forest model, as this model results in the largest reduction of friction velocity at AC (see Figure 4).

Secondary effects are caused by variations in humidity deficit. After an infinitely long fetch, the simulated humidity deficit over the forest slightly exceeds the adjusted value over AC. This effect is caused by the relatively large stomatal resistance of the forest. At limited fetch, the forest is exposed to a humidity deficit slightly below the adjusted value and thus the evaporation is further reduced. In the multi-layer approach, the leaves are situated at some height above the soil surface, resulting in a further reduction of humidity deficit and transpiration at small fetches. At small fetches, AC is exposed to a humidity deficit slightly exceeding the value after a long fetch, but this variation of humidity hardly influences transpiration, due to the limited exchange between AC and the atmosphere. In the case of the multilayer approach, the friction velocity above AC is so small that the effect of humidity on transpiration is overshadowed by the already mentioned effect of net radiation. The simulated similarity of the humidity deficits above forest and AC is in agreement with observations of Pearce *et al.* (1980) in non-rainy situations.

Figure 7 shows the average regional evaporation as a function of regional length scale l_r (the distances in the wind direction across both forest and AC) for a region with 50% fractional cover of forest. For instance, at $l_r = 1$ km this figure shows the average evaporation of Figure 6. Local advection appears to reduce regional

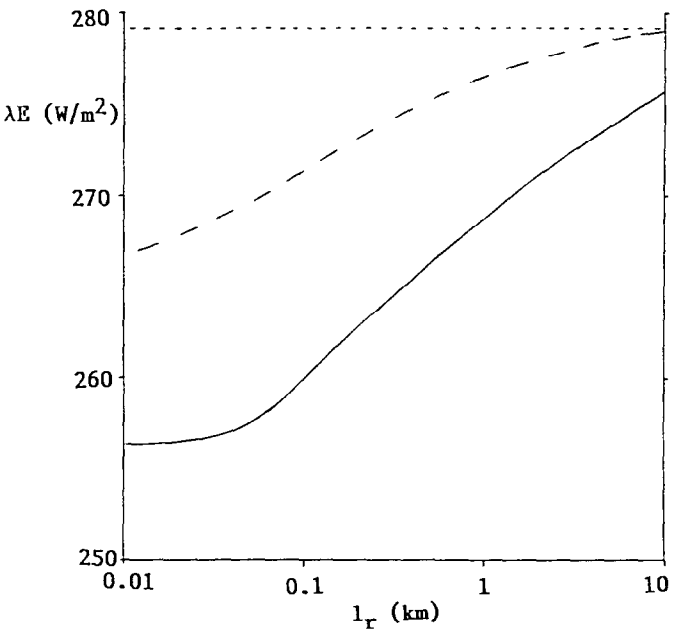

Fig. 7. Transpiration of a region of 50% forest and 50% agricultural land versus regional length scale, using the same symbols as Figure 6.

evaporation in this case, especially when the multi-layer model is used. Regional evaporation flux is reduced most for small regions (i.e., many transitions between forest and AC), but even for the largest region simulated, the effects are still obvious.

Figure 8 shows that the regional momentum flux is increased, in particular when the multi-layer model is used. This result is caused by the strong increase of momentum flux (the square of friction velocity) at the upwind forest edge (Figure 3) in combination with the limited reduction of momentum flux in the lee of the forest (Figure 4).

For lengths l_r of only some tens of meters a situation arises that is commonly denoted as 'open forest' or 'sparse vegetation'. Here the open space between the trees is of the same order of magnitude as their height. Figures 7 and 8 show that the fluxes of open forest are almost independent of the l_r, and only dependent on the fractional cover when the multi-layer model is used. However, for given tree sizes, the fractional cover depends on tree spacing.

Figure 8 shows that the momentum flux of forest with reduced leaf area index is increased; this is in agreement with the increased roughness length, as discussed in Section 2.5. Figure 8 also shows that the momentum flux of open forest is larger than the flux of a closed forest with the same leaf area index. The relatively large momentum flux above irregular forest is caused by the exponential reduction of mixing length by leaves (Equation (23)); thus clustered leaves result in a smaller

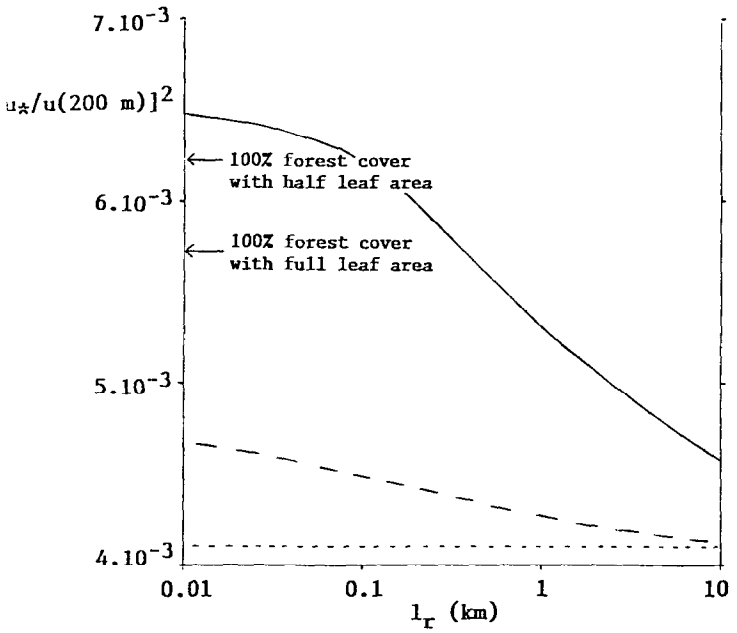

Fig. 8. As Figure 7 for the scaled momentum flux. The figure also shows the scaled momentum fluxes of homogeneous regions with 100% forest cover for two leaf area indices. According to the multi-layer model, the scaled momentum flux for small l_r (many transitions between forest and grassland) exceeds the values of a completely forested region, as explained in the text.

reduction of mixing length and the atmospheric exchange is more efficient. This result is in agreement with the large roughness length obtained by Fazu and Schwerdtfeger (1989) and the deviation in the flux-profile relation obtained by Garratt (1978) and Högström *et al.* (1989) for open forest.

Evaporation and momentum flux versus fractional cover are shown in Figures 9 and 10. The decrease of evaporation and increase of momentum flux, due to local advection, is in agreement with Figures 7 and 8. Figures 9 and 10 show that the influence of local advection is particularly important when only a small fraction of the region is forested. Such a region is commonly denoted as a region with windbreaks. The strong increase of momentum flux when windbreaks are added to a region is in agreement with measurements of Seguin and Gignoux (1974). In a region with multiple windbreaks, these authors measured a regional roughness length that is typical for a forest of the same height. This result can only be understood using a multi-layer model.

4.2. Partially irrigated regions

The average evaporation of a region with 50% irrigated rice cover and 50% dry bare soil is shown in Figure 11. The average evaporation increases when the regional length scale decreases and reaches a limiting value at the open canopy scale. As discussed in Section 3.2, the deviation between the single and multi-

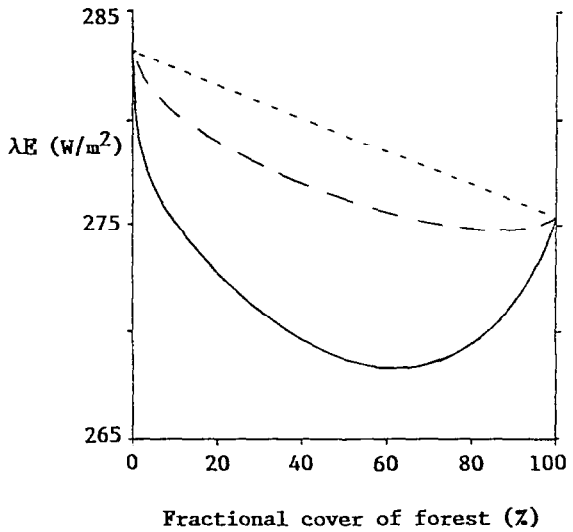

Fig. 9. Transpiration versus fractional forest cover for $l_r = 1$ km with the remaining part covered by agricultural land, using the symbols of Figure 6.

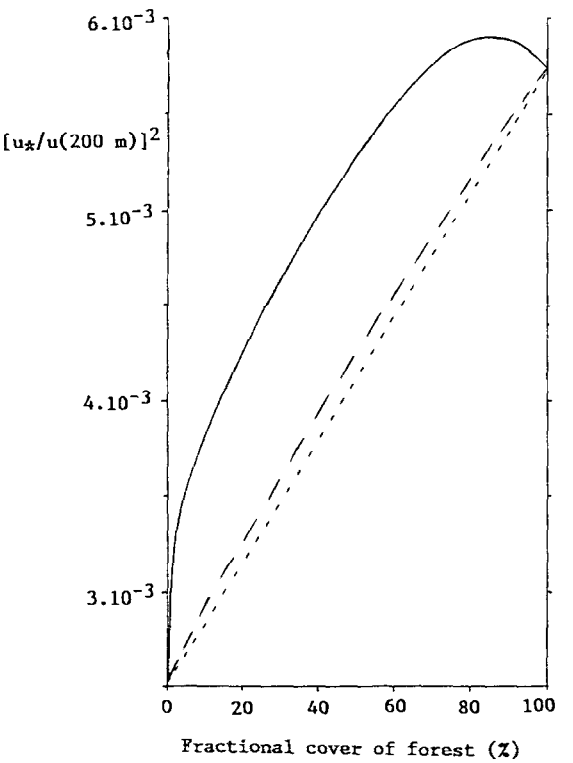

Fig. 10. As Figure 9, for the scaled momentum flux, using the symbols of Figure 6.

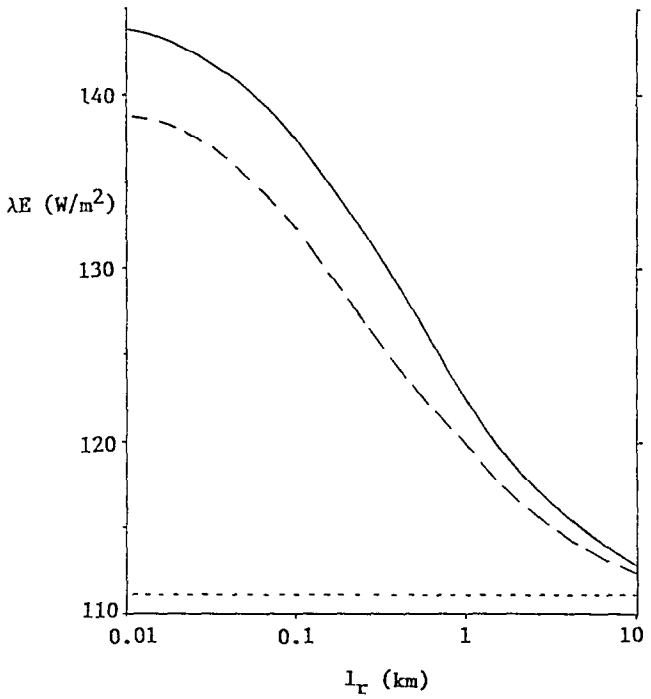

Fig. 11. Transpiration of a region of 50% irrigated rice and 50% dry bare soil versus l_r; as in Figure 6, the following symbols are used: —— = multilayer model, ----- = single-layer model and ---- = without local advection.

layer model is small in this case, because a stable atmospheric layer is formed in the upper part of the canopy.

The regional momentum flux is increased for small-scale regions, especially when using the multi-layer model (Figure 12). The increase of momentum flux was already discussed in connection with Figure 8, and both figures are compared in the following section.

At a regional length scale of 1 km, local advection effects are of similar significance as a 10% change in fractional cover, to the average fluxes (Figures 13 and 14).

5. Discussion: Regional Consequences of Local Advection

Regional consequences of local advection emerge from the calculated flux differences with and without local advection (Figures 7–14). The situation without local advection is defined here as a situation where wind velocity, air temperature and humidity are horizontally constant at the top of the surface layer (no regional advection), and are immediately adjusted to the underlying surface, using the common flux-profile relations Equations (18)–(20) up to the top of the surface

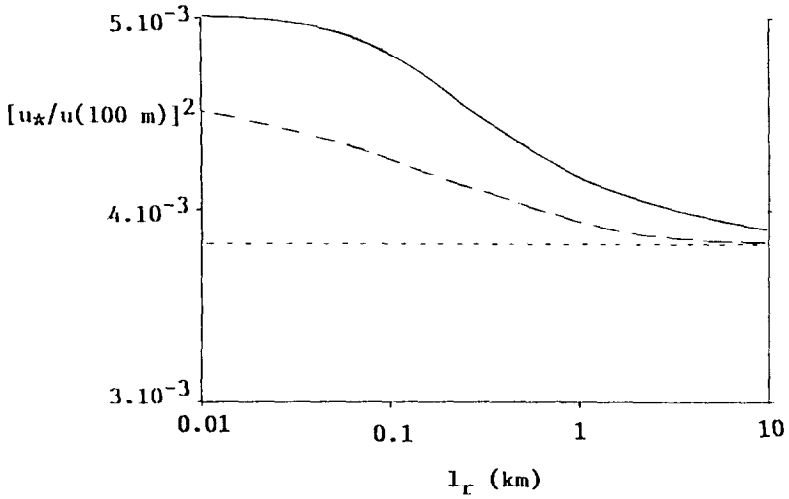

Fig. 12. As Figure 11, for the scaled momentum flux.

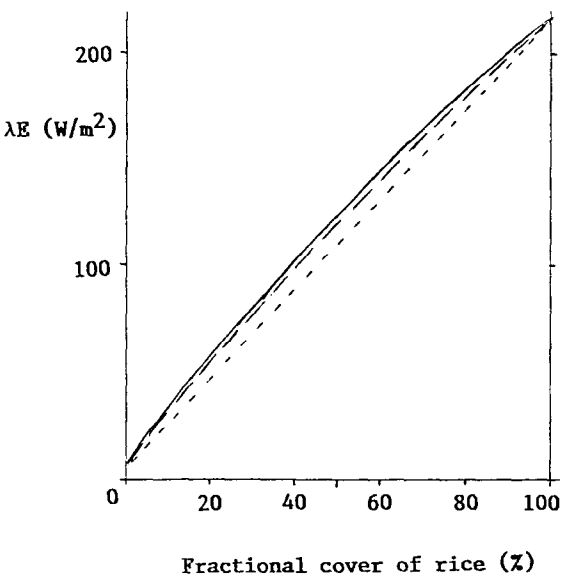

Fig. 13. Transpiration versus fractional cover of the irrigated rice for a region of 1 km length scale with the remaining part covered with bare soil, using the symbols of Figure 11.

layer. The top of the surface layer is situated at 100 m height in the partially irrigated region, and at 200 m in the partially forested region (Table I).

The single-layer vegetation model shows similar effects of local advection on regional fluxes as found by Mason (1988) and Claussen (1991). Their results are also based on a single-layer surface model. Figures 3 and 4 show that the multi-layer vegetation model simulates the fluxes near edges of tall vegetation more accurately, so the results of this version of the model will be emphasized. Using

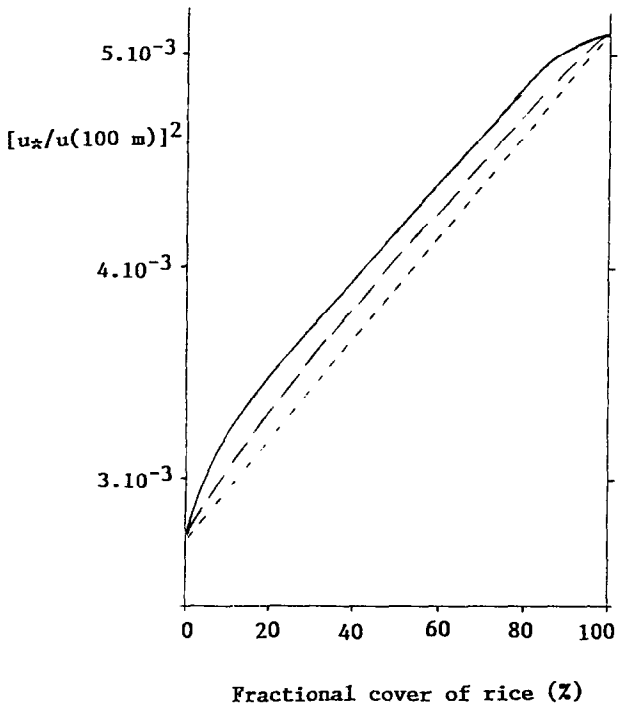

Fig. 14. As Figure 13, for the scaled momentum flux.

the multi-layer model, Figure 8 shows that local advection may increase regional momentum flux by up to 50%. Consequently it is important to incorporate local advection in the surface flux calculation method of meso-scale models.

Averaging rules for local advection can be obtained from an accurate, well validated surface-layer model. The present model is sufficiently validated to analyse the regional effects of local advection qualitatively.

Figures 8, 10, 12 and 14 show that regionally averaged momentum flux is increased by local advection, which is in qualitative agreement with studies by André and Blondin (1986), Taylor (1987), Mason (1988) and Claussen (1991). The physical explanation of the momentum flux increase by local advection is that in the case of a variable surface roughness, the rougher zone is exposed to higher wind speeds and the smoother zone to lower wind speeds relative to the adjusted flow. So a positive correlation is found between roughness and perturbations from adjusted windspeed. This quadratic effect on friction velocity perturbations implies that the increase of the fetch-averaged momentum flux in the rougher zone exceeds the decrease in the smoother zone, and results in an increased ratio between friction velocity and windspeed at the top of the surface layer.

A perturbation analysis regarding the consequence of local advection on regional evaporation in a situation of constant surface roughness, has been given by McNaughton (1976). Relatively small deviations of stomatal resistance appear to

result in enhanced differences in evaporation downwind of the edge, that nearly compensate on a regional scale. In the case of one very dry zone, regional evaporation is increased as the flux perturbations are concentrated in the wet zone (Figure 5, 11 and 13). Momentum flux perturbations may decrease regional evaporation (Figures 6, 7 and 9), but the sign of this effect depends mainly on the difference between actual and equilibrium evaporation (Section 4.1). In summary, regional evaporation may increase as well as decrease as a result of local advection, due to the combined effects of local variations in stomatal resistance and surface roughness, whereas regional momentum flux is always increased by variations in surface roughness.

The significance of local advection on regional fluxes depends on the heterogeneity of the region. According to Figures 7, 8, 11 and 12, the significance increases for decreasing l_r or decreasing distances between vegetation edges in the direction of the wind. For the open canopy length scale, at very small l_r, the regional fluxes are almost independent of l_r. With increasing l_r, the fluxes gradually change until local advection becomes insignificant for the regional fluxes.

Gradual change of flux is encountered between 0.1 and 10 km for forest (Figures 7 and 8) and between 0.01 and 1 km for rice (Figures 11 and 12). By scaling with the height difference between the tall and short vegetation in the region, δh_c, the change is found for $10\delta h_c < l_r < 10^3 \delta h_c$. These simulation results indicate that $\delta h_c / l_r$ is a measure of surface heterogeneity due to vegetation edges. Scaling heterogeneity with $\delta h_c / l_r$ is in agreement with scaling practices in wind-break technology (see review by McNaughton, 1989) and similar to fetch-to-height requirements for flux observations in heterogeneous regions (Rosenberg *et al.*, 1983).

The simulated regional fluxes are sensitive to local advection as long as $l_r < 10^3 \delta h_c$. The factor 10^3 is an order of magnitude larger than used in wind-break design and fetch-to-height measurement requirements. This difference was already noticed in Section 3.2. The measurements of G86 on heath were made at a fetch where the flux is constant up to the measurement height, but the wind velocity still increases slowly with fetch (Figure 4). The significance of gradual changes at large fetches appears from the differences between the 'heath' and 'clearing' simulation (Figure 3). The gradual changes at large fetches imply that (1) measurements are influenced by an upwind region exceeding the common fetch-to-height ratio, and (2) even sparse heterogeneities may influence the average fluxes.

6. Conclusions

By taking advection of mixing length into account, the momentum flux of the surface after a step change in surface roughness or vegetation cover can be determined accurately using a simple mixing-length closure. The mixing length adjusts only slowly to the new surface.

A simple function for the reduction of mixing length by leaf area density

yields promising results for the estimation of roughness length and zero-plane displacement of vegetation. It can also explain the relatively large roughness of heterogeneous 'open' vegetation.

The single-layer 'big leaf' representation of vegetation, although adequate for homogeneous surfaces, underestimates local advection near edges of vegetation. The underestimation is mainly caused by the neglect of air flow into the vegetation and flow out of the vegetation at the lee side.

According to the multi-layer vegetation model, local advection increases regional momentum flux by up to 50% of the value that would be obtained at immediate adjustment of the surface layer. Consequently, local advection is significant for meso-scale modelling. Regional evaporation seems to be less sensitive and may increase as well as decrease because of local advection. The simulations suggest that even very widely spaced heterogeneities in vegetation height influence regional fluxes.

According to the present simulations, regional fluxes are more sensitive to local advection than previously assumed from single-layer simulations. The discrepancy implies that local advection is still poorly understood. Further theoretical and observational studies on average fluxes from regions between the micro- and meso-scale are recommended.

Acknowledgements

This study has been executed in cooperation with A. W. L. Veen, B. Kruijt and R. W. A. Hutjes from the forest water dynamics group of our department. Stimulating discussions were held with M. Claussen, GKSS Forschungszentrum Geesthacht, BRD. Observations were made available by J. H. C. Gash and H. R. Oliver, Institute of Hydrology, UK. A. J. Dolman of the same institute examined a preliminary draft of this paper critically.

References

André, J. C. and Blondin, C.: 1986, 'On the Effective Roughness Length for Use in Numerical Three-Dimensional Models', *Boundary-Layer Meteorol.* **35**, 231–245.

André, J. C., Goutorbe, J. P., and Perrier, A.: 1986, 'HAPEX-MOBILHY, a Hydrologic Atmospheric Pilot Experiment for the Study of Water Budget and Evaporation Flux at the Climatic Scale', *Bull. Amer. Meteorol. Soc.* **67**, 138–144.

André, J. C., Bougeault, P., and Goutorbe, J. P.: 1990, 'Regional Estimates of Heat and Evaporation Fluxes over Non-Homogeneous Terrain, Examples from the HAPEX-MOBILHY Programme', *Boundary-Layer Meteorol.* **50**, 77–108.

Avissar, R. and Verstraete, M. M.: 1990, 'The Representation of Continental Surface Processes in Atmospheric Models', *Rev. Geophysics* **28**, 35–52.

Baldocchi, D. D., Matt, D. R., Hutchison, B. A., and McMillen, R. T.: 1984, 'Solar Radiation within an Oak-Hickory Forest: An Evaluation of the Extinction Coefficients for Several Radiation Components During Fully Leaved and Leafless Periods', *Agric. Forest Meteorol.* **32**, 307–322.

Baldocchi, D. D. and Meyers, T. P.: 1988, 'A Spectral and Lag-Correlation Analysis of Turbulence in a Deciduous Forest Canopy', *Boundary-Layer Meterol.* **45**, 31–58.

Betts, A. K., Desjardins, R. L., MacPherson, J. I., and Kelly, R. D.: 1990, 'Boundary Layer Heat and Moisture Budgets from FIFE', *Boundary-Layer Meteorol.* **50**, 109–138.

Blackadar, A. K.: 1962, 'The Vertical Distribution of Wind and Turbulent Exchange in a Neutral Atmosphere', *J. Geophys. Res.* **67**, 3095–3102.

Bradley, E. F.: 1968, 'A Micrometeorological Study of Velocity Profiles and Surface Drag in the Region Modified by a Change in Surface Roughness', *Quart. J. Roy. Meteorol. Soc.* **94**, 361–379.

Brakke T. W., Verma, S. B., and Rosenberg, N. J.: 1978, 'Local and Regional Components of Sensible Heat Advection', *J. Appl. Meteorol.* **17**, 955–963.

Bruin, H. A. R. de and Holtslag, A. A. M.: 1982, 'A Simple Parameterization of the Surface Fluxes of Sensible and Latent Heat with the Penman-Monteith Concept', *J. Appl. Meteorol.* **21**, 1610–1621.

Claussen, M.: 1988, 'Models of Eddy Viscosity for Numerical Simulation of Horizontally Inhomogeneous, Neutral Surface Layer Flow', *Boundary-Layer Meteorol.* **42**, 337–369.

Claussen, M.: 1991, 'Estimation of Areally-Averaged Surface Fluxes', *Boundary Layer Meteorol.* **54**, 387–410.

Crout, N. M. J., Gregson, K., and Unsworth, M. H.: 1990, 'TLM: A Technique with Application in the Numerical Solution of Diffusion Problems', *Agric. Forest Meterol.* **51**, 1–20.

Fazu, C. and Schwerdtfeger, P.: 1989, 'Flux-Gradient Relations for Momentum and Heat Over a Rough Natural Surface', *Quart. J. Roy. Meteorol. Soc.* **115**, 335–352.

Garratt, J. R.: 1978, 'Flux-Profile Relations above Tall Vegetation', *Quart. J. Roy. Meteorol. Soc.* **104**, 199–211.

Garratt, J. R. and Francey, R. J.: 1978, 'Bulk Characteristics of Heat Transfer in the Baroclinic Atmospheric Boundary Layer', *Boundary-Layer Meteorol.* **15**, 399–421.

Garratt, J. R. and Pielke, R. A.: 1989, 'On the Sensitivity of Mesoscale Models to Surface-Layer Parameterization Constants', *Boundary-Layer Meteorol.* **48**, 377–397.

Gash, J. H. C.: 1986, 'Observations of Turbulence Downwind of a Forest-Heath Interface', *Boundary-Layer Meteorol.* **36**, 227–237.

Högström, U., Bergström, H., Smedman, A., Halldin, S., and Lindroth, A.: 1989, 'Turbulent Exchange Above a Pine Forest. I: Fluxes and Gradients', *Boundary-Layer Meteorol.* **49**, 197–217.

Hutjes, R. W. A., Klaassen, W., Kruijt, B., and Veen, A. W. L.: 1991, 'Predicting Near-Surface Meteorological Variations over Different Vegetation Types', Accepted by Proc. XX Gen. Assembly IUGG, IAHS, Vienna.

Jarvis, P. G., James, G. B., and Landsberg, J. J.: 1976, 'Coniferous Forest. in J. L. Monteith (ed.), *Vegetation and the Atmosphere*, Vol. 2, Academic Press, pp. 171–240.

Jarvis, P. G. and Leverenz, J. W.: 1983, 'Productivity of Temperate, Deciduous and Evergreen Forests. in O. L. Lange, P. S. Nobel, C. B. Osmond, and H. Ziegler (eds.), *Encyclopedia of Plant Physiology*, Vol. 12D. Springer Verlag, pp. 233–280.

Jarvis, P. G. and McNaughton, K. G.: 1986, 'Stomatal Control of Transpiration: Scaling Up from Leaf to Region', *Adv. Ecol. Res.* **15**, 1–49.

Kim, J., Verma, S. B., and Rosenberg, N. J.: 1989, 'Energy Balance and Water Use of Cereal Crops', *Agric. Forest Meteorol.* **48**, 135–147.

Kruijt, B., Klaassen, W., Hutjes, R. W. A., and Veen, A. W. L.: 1991: 'Heat and Momentum Fluxes Near a Forest Edge', Accepted by Proc. XX Gen. Assembly IUGG, IAHS, Vienna.

Lang, A. R. G., Evans, G. N., and Ho, P. Y.: 1974, 'The Influence of Local Advection on Evapotranspiration from Irrigated Rice in a Semi-Arid Region', *Agric. Meteorol.* **13**, 5–13.

Lang, A. R. G., McNaughton, K. G., Fazu, C., Bradley, E. F., and Ohtaki, E.: 1983, 'Inequality of Eddy Transfer Coefficients for Vertical Transport of Sensible and Latent Heat Flux During Advective Inversions', *Boundary Layer Meteorol.* **25**, 25–41.

Li, Z., Miller, D. R., and Lin, J. D.: 1985, 'A First Order Closure Scheme to Describe Countergradient Momentum Transport in Plant Canopies', *Boundary-Layer Meteorol.* **33**, 77–83.

Li, Z., Lin, J. D., and Miller, D. R.: 1990, 'Air Flow Over and Through a Forest Edge: A Steady-State Numerical Simulation', *Boundary-Layer Meteorol.* **51**, 179–197.

Mason, P. J.: 1988, The Formation of Areally Averaged Roughness Lengths', *Quart. J. Meteorol. Soc.* **114**, 399–420.

McNaughton, K. G.: 1976, 'Evaporation and Advection II: Evaporation Downwind of a Boundary Separating Regions Having Different Surface Resistances and Available Energies', *Quart. J. Roy. Meteorol. Soc.* **102**, 193–202.

McNaughton, K. G.: 1983, 'The Direct Effect of Shelter on Evaporation Rates: Theory and an Experimental Test', *Agric. Meteorol.* **29**, 125–136.

McNaughton, K. G.: 1988, 'Effects of Windbreaks on Turbulent Transport and Microclimate', *Agric. Ecosystems Environ.* **22–23**, 17–39.

Monteith, J. L.: 1973, *Principles of Environmental Physics*, London: Edward Arnold.

Monteith, J. L.: 1965, 'Evaporation and Environment', in G. E. Fogg (ed.), The State and Movement of Water in Living Organisms', *Soc. Exptl. Biol. Symp.*, **19**, 205–234.

Pearce, A. J., Gash, J. H. C., and Stewart, J. B.: 1980, 'Rainfall Interception in a Forest Stand Estimated from Grassland Meteorological Data', *J. Hydrol.* **46**, 147–163.

Pearman, G. I., Weaver, H. L., and Tanner, C.: 1972, 'Boundary Layer Heat Transfer Coefficients', *Agric. Meteorol.* **10**, 83–92.

Pinty, J-P, Mascart, Richard, E., and Rosset, R.: 1989, 'An Investigation of Mesoscale Flows Induced by Vegetation Inhomogeneities Using an Evapotranspiration Model Calibrated Against HAPEX-MOBILHY Data', *J. Appl. Meteorol.* **28**, 976–992.

Raupach, M. R. and Thom, A. S.: 1981, 'Turbulence in and Above Plant Canopies', *Ann. Rev. Fluid Mech.* **13**, 97–129.

Rosenberg, N. J., Blad, B. L., and Verma, S. B.: 1983, *Micro-climate: The Biological Environment*. Wiley, New York, 495 pp.

Seguin, B. and N. Gignoux, N.: 1974, 'An Experimental Study of Wind Profile Modification by a Network of Shelterbelts', *Agric. Meteorol.* **13**, 15–23 (in French).

Shaw, R. H. and Perreira, A. R.: 1982, 'Aerodynamic Roughness of a Plant Canopy: A Numerical Experiment', *Agric. Meteorol.* **26**, 51–65.

Shuttleworth, J. W.: 1988, 'Macrohydrology – The New Challenge for Process Hydrology', *J. Hydrology* **100**, 31–56.

Shuttleworth, W. J., 1989: Micrometeorology of Forests. in P. G. Jarvis, J. L. Monteith, W. J. Shuttleworth, and M. H. Unsworth (eds.), *Forests, Weather and Climate*. The Royal Society London, pp. 125–156.

Spittlehouse, D. L. and Black, T. A.: 1982, A Growing Season Water Balance Model Used to Partition Water Use Between Trees and Understory. In: *Proc. of Canadian Hydrol. Symp.* **82**, 195–214. Ottawa, Ass Comm. Hydrol., Nat. Res. Council.

Taylor, P.: 1987, 'Comments and Further Analysis on Effective Roughness Length for Use in Three Dimensional Models', *Boundary-Layer Meteorol.* **39**, 403–418.

Veen, A. W. L. and Dolman, A. J.: 1989, 'Water Dynamics of Forests: One-Dimensional Modelling', *Prog. Phys. Geogr.* **13**, 471–506.

Verma, S. B., Baldocchi, D. D., Anderson, E. E., Matt, D. R., and Clement, R. J.: 1986, 'Eddy Fluxes of CO_2, Water Vapour and Sensible Heat Over a Deciduous Forest', *Boundary-Layer Meteorol.* **36**, 71–91.

Webb, E. K.: 1970, Profile Relationships: The Log-Linear Range and Extension to Strong Stability', *Quart. J. Roy. Meteorol. Soc.* **96**, 67–90.

Webb, E. K.: 1982, 'Profile Relationships in the Superadiabatic Surface Layer', *Quart. J. Roy. Meteorol. Soc.* **108**, 661–688.